Journal of Computer-Aided Molecular Design, **12:** 533–542, 1998.
KLUWER/ESCOM

Elucidation of a common structure of selective fibrinogen receptor antagonists

Hervé Minoux[a], Nicolas Moitessier[b], Yves Chapleur[b] & Bernard Maigret[a]
[a]*Groupe Biochimie Théorique, and* [b]*Groupe SUCRES, U.M.R. CNRS 7565, Université Henri Poincaré, Nancy I, BP 239, F-54506 Vandoeuvre-lès-Nancy Cedex, France*

Received 22 September 1997; Accepted 27 April 1998

Key words: $\alpha_{IIb}\beta_3$ integrin, molecular modelling, RGD

Summary

In this paper, we investigate the common structural and electrostatic parameters of a series of specific inhibitors of the $\alpha_{IIb}\beta_3$ integrin. Molecular dynamics simulations with an explicit aqueous environment led to an original theoretical pattern. Our results may suggest that the studied non-peptide $\alpha_{IIb}\beta_3$ antagonists developed upon the Arg-Gly-Asp ubiquitous recognition sequence, in fact, should mimic the C-terminus part of the fibrinogen γ chain. This assumption could, therefore, explain their specificity with respect to other Arg-Gly-Asp-dependent integrins.

Introduction

When a blood vessel is injured, platelets are activated to adhere to the disrupted surface and to each other, leading to the development of aggregates that precedes the formation of a haemostatic plug. Under pathophysiological conditions, however, the thrombus formation in an arterial vessel can be the cause of cardiovascular and cerebrovascular diseases. The binding of fibrinogen to platelets is the final obligatory step in platelet aggregation [1]. The $\alpha_{IIb}\beta_3$ integrin is a saturable fibrinogen receptor on platelets [2], and its blockade might constitute a superior approach in preventing effectively arterial thrombus formation [3, 4]. The amino acid sequence Arg-Gly-Asp (RGD in the one-letter code), contained in many adhesive proteins, has been shown to inhibit the fibrinogen binding to its receptor, and is believed to represent the minimal sequence necessary for binding $\alpha_{IIb}\beta_3$ [1, 2]. Fibrinogen is a dimer of three chains: α, β and γ. Each of the α chain, contains two RGD recognition sequences, i.e., RGDF units at α95–98 and RGDS units at α572–575 [5–8]. It also contains a $\alpha_{IIb}\beta_3$ specific recognition sequence: the dodecapeptide C-terminus of each of its γ chains, which cross-links the α_{IIb} subunit at 294–314 [9–12]. Although the RGD tripeptide is sufficient to inhibit platelet aggregation, other inhibitors of the interaction between fibrinogen and $\alpha_{IIb}\beta_3$ have been developed: monoclonal antibodies, linear and cyclic peptides containing RGD, peptidomimetics and non-peptide antagonists [13]. Several RGD-based inhibitors, however, block also other integrins, including $\alpha_v\beta_3$, which is widely distributed and plays a major role in cell adhesion, tumor metastasis and bone resorption [14–17].

The purpose of our work is to define the structural and electrostatic parameters required to inhibit potently and specifically platelet aggregation. The use of structure-based design to develop original and bioactive non-peptide compounds is now accepted as one of the most promising way to discover new drugs [18]. This technique requires some knowledge about putative bioactive conformations of known ligands. Nevertheless, since it is often impossible to determine directly the bound state structure of these ligands, the definition of consensus conformations in solution of some potent compounds could be another way to obtain information about the structural parameters that are required for activity. In this paper, such an approach is used to propose a theoretical pattern for a hypothetical bioactive conformation of specific and potent fibrinogen receptor antagonists.

Materials and methods

All calculations and analyses were performed with the Biosym/MSI molecular modelling package [19]. They were carried out using the CVFF force field, in which off-diagonal terms were not taken into account and Morse functions were replaced by harmonic ones.

The aim of this study is to determine the conformational behaviour of the selected molecules in water. Our method involves three steps:
– first, a preliminary conformational sampling, using simulated annealing;
– second, a molecular dynamics simulation with explicit water molecules around the studied antagonist.
– third, a conformational analysis from the molecular dynamics trajectory.

Conformational sampling

For each investigated compound, a starting conformation was first built and refined by 1000 steps of energy minimization using a conjugate gradient algorithm. These starting conformations were then used for a pseudo-simulated annealing conformational sampling [20]; simulated annealing involves a temperature increase of the system, followed by a slow cooling to avoid local minima, thereby trying to locate the global minimum region of the energy function. This conformational sampling was performed using molecular dynamics (MD) in a vacuum (over 40 000 steps with a timestep of 1 fs). The equations of motion were integrated using the Leapfrog version of the Verlet algorithm [21]. The dielectric constant used was distance-dependent ($\epsilon = r$) to simulate roughly the electrostatic shielding due to the solvent. The (*N*, *V*, *T*) ensemble was used at a fixed value, with the Berendsen algorithm. This method allows to maintain temperature, at a fixed value by means of a coupling to an external bath. The simulated annealing-like method used here consists of one hundred loops of slow cooling, each one leading to a low energy conformation. Each loop begins by fixing the temperature to 1000 K, followed by 5000 steps of MD. The temperature was then decreased by steps of 100 K. Decreasing the temperature by 100 K every 5000 steps, so that after 40 000 steps, the temperature of the system corresponds approximately to 300 K. The final conformation obtained at the end of this process was energy-refined using a conjugate gradient algorithm, and, after storage, was used to start a new simulation at high temperature with a slow cooling stage, as described above. This procedure produced 100 minimized conformations for each molecule. Among those, the 20–30 lowest energy structures were selected and gathered into conformational families. To test the validity of this conformational sampling method, it was repeated for one given compound, and the resulting conformational families were compared and found to be similar.

Molecular dynamics in an aqueous solution

The most stable conformation from each structural family obtained from the sampling stage was placed at the centre of a cubic box filled with water molecules. The length of the cell was defined to be longer than twice the maximum distance between two atoms of the considered compound. In practice, the cell length ranged from 25 to 40 Å, and the number of water molecules in the boxes varied between 500 and 2000. The water molecules overlapping the studied molecule were removed. The water model used by Biosym/MSI is a three-site hybrid of the TIP3P and the SPC models. Periodic boundary conditions were used. A spherical cut-off corresponding to less than half of the cell length was used to truncate non-bonded interactions, and the dielectric constant value was fixed at 1.0. The (*N*, *P*, *T*) ensemble was used with a temperature fixed at 300 K and a pressure fixed to 1 bar. The Berendsen algorithm was used to maintain both the temperature and the pressure at the desired value. The complete system formed by the antagonist and water, after an energy minimization of 200 steps steepest descents algorithm followed by a conjugate gradient refinement until convergence, was used as a starting point for 10 000 steps of molecular dynamics equilibration. A time step of 1 fs was used. Then, 1 ns of MD trajectory was produced. Configurations were stored every 10 000 steps.

Analysis

For each compound, in order to compare the 100 frames collected during the 1 ns of MD trajectory in water, a cluster diagram was built, with the frames on the *x* and *y* axis, and the root mean square deviation (RMSD) between the two corresponding frames on the *z* axis. The diagram allowed a break-down of the 100 frames into conformational families. For each family, one representative frame was chosen. The RMSD between two frames was calculated using all heavy atoms in the investigated molecule. To ensure that the conformational space was sampled appropriately during the simulation, two MD trajectories of 1 ns each were performed with the same starting conformation

for one compound, but with a different distribution of starting velocities and the same resulting conformational families were obtained. The final step in the analysis consisted of a visual comparison of all representative frames of the studied antagonists. This comparison was carried out by superimposing the different charged groups. The biological activity of these molecules, indeed, seems – at least in part – to be due to the relative positions of these charged groups, as well as the side chain conformation [23, 24]. If this assumption is true, at least one of the selected conformations for each studied molecule, could be superimposed as it adopts the same structure as the other antagonists. In turn, this may imply that the resulting average structure is the bioactive conformation.

We have considered some molecules recently developed by pharmaceutical companies. Our aim is to select the most potent and selective antagonists with respect to the $\alpha_{IIb}\beta_3$ receptor. Among the different $\alpha_{IIb}\beta_3$ low molecular weight antagonists already published, we have chosen the following five:

(**1**) MK 0383, by Merck [25–26];

(**2**) Ro 43-5054 and (**3**) Ro 43-8857, by Hoffman La Roche [27];

(**4**) FR 144633, by Fujisawa [28];

(**5**) KGDW analogue, in fact compound 15 in ref. 29.

The inhibitory capacities (IC_{50}) shown in Figure 1 are the concentrations of antagonists required to achieve 50% inhibition in the number of $\alpha_{IIb}\beta_3$ or $\alpha_v\beta_3$ receptors. These five molecules were developed on different bases (except for Ro 43–5054 and Ro 43–8857 which stemmed from the same study). MK 0383 is the result of the optimisation of a lead compound that has been identified by a directed search of a sample collection for compounds having amino and carboxylate functions separated by through-bond distances of 10–20 Å. This distance requirement is based on the hypothetical spatial separation between the guanidine moiety of Arg and the β-carboxyl moiety of Asp in the RGD sequence [26].

Ro 43–5054 and Ro 43–8857 were developed from the tetrapeptide RGDS, known as a recognition sequence of fibrinogen for the $\alpha_{IIb}\beta_3$ integrin [27].

Compound (**5**) that contains the KGDW sequence was developed during a work investigating the effect of the substitution by lysine or by other homologues of the RGDW sequence concomitantly with an N_α-elongation by non-α-amino acid or piperidinocarboxylic acid. As reported by Scarborough et al. [30, 31], the peptide analogues containing lysine instead of arginine did show an increased selectivity with respect to $\alpha_{IIb}\beta_3$.

No details about the FR 144633 design were found.

The structure of the dodecapeptide C-terminus of the fibrinogen γ chain **(6)** was studied too (HHLGGAKQAGDV in the one-letter amino acid code). This amino acid sequence is known to inhibit specifically platelet aggregation interacting with the α_{IIb} subunit of the $\alpha_{IIb}\beta_3$ integrin [32]. This sequence is active when it is set in the fibrinogen amino acid sequence, but also when it is put alone in solution [9–11].

For the investigated antagonists, the carboxylate moiety was charged, and the *p*-amidinobenzoyl and piperidine groups were protonated. For the dodecapeptide and the KGDW sequence, the lysine was protonated and the aspartic acid was charged. We added a methyl group at the N-terminus and charged the carboxylate on the valine C-terminus. The N- and C-terminus of the KGDW compound were charged too. Except for the dodecapeptide, the partial charges were determined from a Mulliken population analysis after a semi-empirical MNDO calculation [33]. The partial charges of the dodecapeptide were assigned by the *Insight® II* program.

Molecule building, simulated annealing calculations, energy minimizations and analysis were performed on Silicon Graphics Indy workstations. Molecular dynamics simulations were performed on Silicon Graphics Power Indigo^2 workstations and on an SGI Power Challenge Array.

Results

In a first stage, only molecules (**1**) to (**5**) were studied. For (**1**), 24 low-energy structures were extracted from the conformational search by the simulated annealing-like method, which were separated into two families. The highest RMSD between two conformations in each family were 4.28 Å and 4.68 Å – calculated only over heavy atoms. For (**2**), 17 structures were extracted, forming one family with an upper RMSD of 3.91 Å. For (**3**), 18 conformations were found with an upper RMSD of 3.6 Å. For (**4**), 22 structures were found from the conformational search and separated into two families, with the highest RMSD values for each family equal to 2.8 Å and 2.7 Å, respectively. For (**5**), 19 structures were extracted, also forming two families, with the highest RMSD values equal to 4.5 Å and 5.4 Å, respectively. For each of these eight

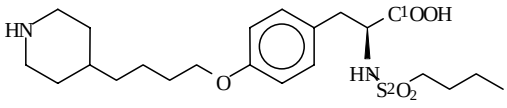

(1) MK0383 :
IC_{50} [$\alpha_{IIb}\beta_3$] = 36 nM
IC_{50} [$\alpha_v\beta_3$] = 0.1 mM

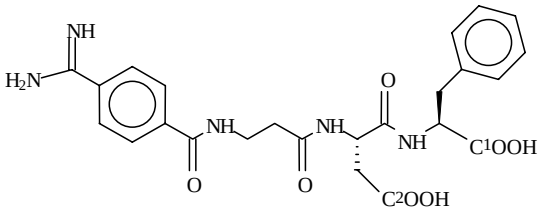

(2) Ro 43-5054 :
IC_{50} [$\alpha_{IIb}\beta_3$] = 60 nM
IC_{50} [$\alpha_v\beta_3$] = 42.3 μM

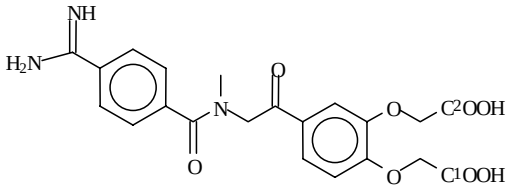

(3) Ro 43-8857 :
IC_{50} [$\alpha_{IIb}\beta_3$] = 70 nM
IC_{50} [$\alpha_v\beta_3$] = 348 μM

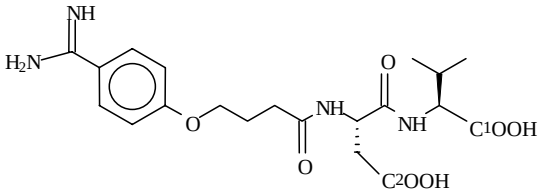

(4) FR 144633 :
IC_{50} [$\alpha_{IIb}\beta_3$] = 78 nM
IC_{50} [$\alpha_v\beta_3$] >1 mM

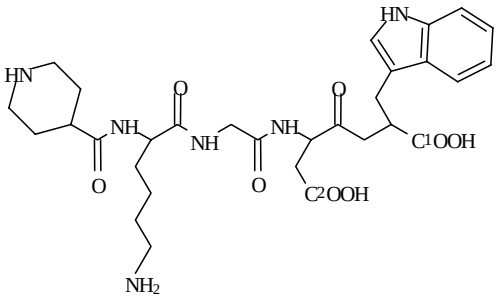

(5) KGDW analogue :
IC_{50} [$\alpha_{IIb}\beta_3$] = 250 nM
IC_{50} [$\alpha_v\beta_3$] > 325 μM

Figure 1. The structures of some $\alpha_{IIb}\beta_3$ selective antagonists; the IC_{50} [$\alpha_{IIb}\beta_3$] values indicate the potency to inhibit platelet aggregation of ADP-activated human (**1**–**4**) or dog (**5**) platelets and the IC_{50} [$\alpha_v\beta_3$] values are the potency to inhibit the vitronectin receptor.

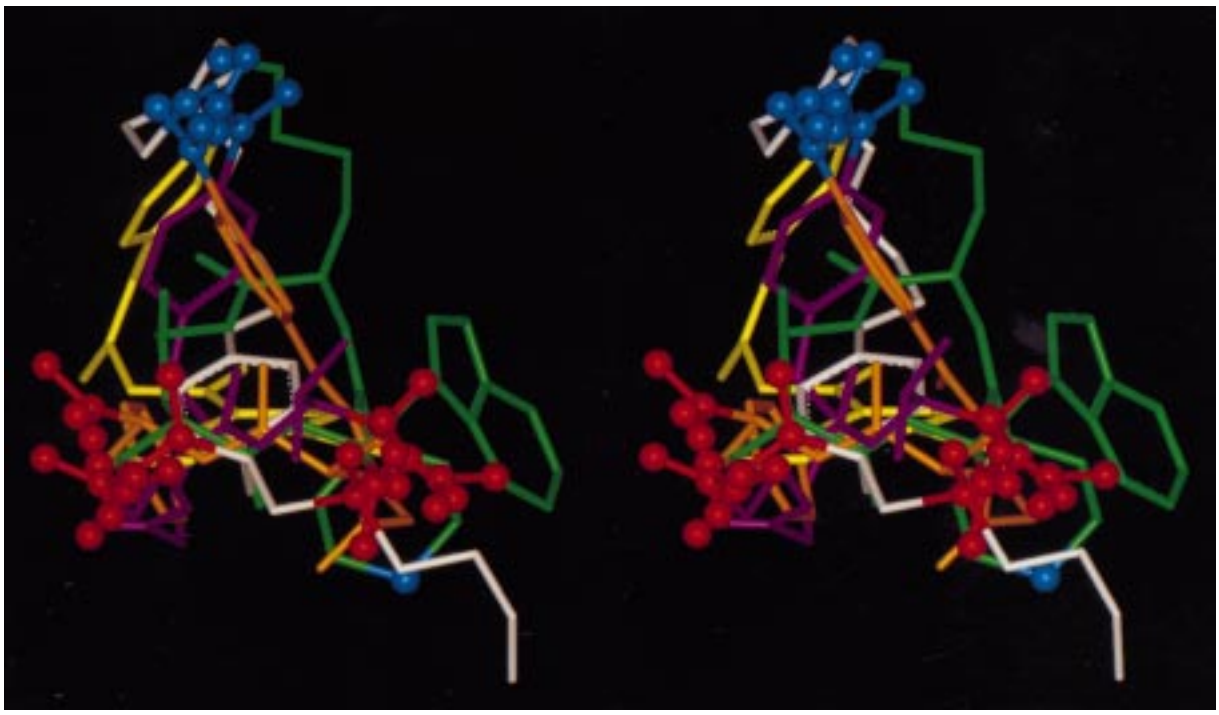

Figure 2. (**1**), (**2**), (**3**), (**4**) and (**5**) superimposed; molecules are coloured according to the following scheme: (**1**) white, (**2**) orange (**3**) yellow, (**4**) purple and (**5**) green. The positive moieties are coloured blue, carboxylate and sulfone moieties are coloured red.

families, the lowest-energy structure was put in a box of water for an MD simulation of 1 ns. The two MD simulations of (**1**) provided 9 structural families, the one of (**2**) provided two families, the one of (**3**) provided two families, those of (**4**) provided 7 families and those of (**5**) provided 5 families. The visual superimposition of all representatives from each family allowed us to divide these frames into three groups. Only one of them contains at least one conformer of the 5 studied molecules, so that this family was supposed to contain the active conformations population. A visual inspection of this family led us to select only one frame for each molecule and to superimpose it with the other selected frames in the best possible manner (see Figure 2).

Based on the assumption that adequate distances between the charged moieties present in each compound are a necessary requirement for the inhibitory activity [23, 24], comparisons between such distances were recorded during the MD simulations and are presented in Figure 3 for all compounds. The considered atoms to compare the distances were: nitrogen for the piperidine or amine moieties, the non-aromatic carbon for the benzamidine group, the carbon atom of the carboxylate moiety and the sulphur atom of the sulfone group. The two distances between each of the two negatively charged group and the positively charged moiety present a common range, viz. from 5.3 to 6.5 Å for the first distance and from 6.2 to 9.3 Å for the second one. The first distance corresponds to the negatively charged moiety near a hydrophobic group. For (**5**), which possesses two positively charged moieties, both were considered during the superimposition step and the group fitting the best to the other antagonists was lysine.

No common range appears clearly for the distance between the two negatively charged groups. At least one conformation of each molecule could, however, be found when considering a range from 4 to 7 Å. From all these boundary distances, a theoretical pattern was built, involving three charged groups, a hydrophobic moiety, and a 'cup-shaped' side chain, linking up these groups (see Figure 4). It is difficult to provide accurate geometrical information about this side chain that looks like an '*open sugar tongs*', but the average shape appears obvious in Figure 2. In addition, and especially for the four non-peptide $\alpha_{IIb}\beta_3$ antagonists, this side chain contains hydrophobic groups.

In a second stage, a conformational study of the dodecapeptide C-terminus of the fibrinogen γ chain

was carried out. Unlike the previous antagonists of the integrin $\alpha_{IIb}\beta_3$, the starting conformation for the MD simulation in a box of water of this short peptide was extracted from a crystal structure of the last 14 residues of the C-terminal part of the fibrinogen γ chain [34]. Four conformational families were extracted from the 1 ns MD trajectory with water molecules. The distances between the three charged moieties of Lys^{406}, Asp^{410} and Val^{411} during the MD simulation are shown in Figure 3, and compared to those of the other antagonists of $\alpha_{IIb}\beta_3$.

When the three charged moieties of a dodecapeptide conformation from one of the four structural families were superimposed on the charged groups of the $\alpha_{IIb}\beta_3$ antagonists shown in Figure 2, a 'cup shaped' side chain between the charged groups of the dodecapeptide could be observed. Thus, it appears that the KQAGDV sequence C-terminus of the fibrinogen γ chain could adopt the same '*open sugar tongs*' structure adopted by the five other antagonists studied here. The duration of the MD simulation is, nevertheless, too short to determine all the solution structures of this highly flexible peptide [35]. Thus, the results of the MD simulation for the dodecapeptide were not used to build the theoretical pattern shown in Figure 4, even if one type of the four structures found is similar to the common structure of the other antagonists of $\alpha_{IIb}\beta_3$. The energy required to convert the random solution structure of (**6**) to the bound conformation is, therefore, higher than the one required for the low molecular weight antagonists (**1**)–(**5**), and could explain the difference between the IC_{50} values of (**1**)–(**5**) – nanomolar scale – and the one of (**6**) – micromolar scale.

Discussion

The discovery that the tripeptide sequence RGD can inhibit platelet aggregation had led to the design of many peptide and non-peptide molecules [13]. The six molecules studied here were chosen according to their highly potent and selective inhibitory capacity with respect to the $\alpha_{IIb}\beta_3$ receptor, and it was assumed that the four non-peptide molecules mimicked the well known RGD sequence. Nevertheless, no assumption was made upon the selectivity of these antagonists: actually, most of the $\alpha_{IIb}\beta_3$ antagonists developed from the RGD sequence during the last ten years were not specific to this integrin and could inhibit other integrins, especially another β_3 integrin: $\alpha_v\beta_3$ which is widely expressed and recognize many ligands, including fibrinogen. This is due to the fact that many integrins bind to the common recognition sequence RGD present in their agonists – or antagonists.

During the design of (**2**) and (**3**), Alig et al. have observed that the specificity appeared when a second carboxylate moiety was added to a non-specific molecule [27]. In fact, when the five first studied molecules were observed, the structural and electrostatic common parameters appearing were: (i) one positively charged moiety (except for (**5**) which possesses 2 of them); (ii) one carboxylate moiety near a hydrophobic group – except for (**3**), which does not possess a hydrophobic group on this site; (iii) another carboxylate moiety or sulfone moiety mimicking this group in the case of (**1**).

On the other hand, the RGD sequence presents only one positively charged group (the guanidinium moiety located at the arginine side chain extremity) and one carboxylate moiety (on the aspartic acid side chain).

Thus, even if a part of the electrostatic and structural properties from the five first studied antagonists is common to these from the Arg-Gly-Asp sequence, it does not necessarily imply that these molecules mimic this sequence.

In fact, when some solvated conformations of (**1**) to (**6**) obtained from the MD simulations were well superimposed (Figure 5), the structure/activity relationship can be interpreted such as all these molecules mimic the binding sequence of the natural agonist, i.e. the hexapeptide C-terminus of the fibrinogen γ chain. This could explain the high selectivity of these antagonists with respect to other RGD-dependent integrins.

Considering that compound (**5**), however, was developed according to the amino acid sequence present in barbourin (a protein extract from a snake venom and known to inhibit specifically platelet aggregation [36]), this cannot explain the specificity of this disintegrin. In fact, its biological activity and specificity might depend not only on the studied KGDW sequence, but on other amino acids present in the protein.

To explain the lack of common gap with the distances between the two negatively charged moieties of the six studied antagonists (see Figure 3, bottom), another assumption can be made: the lack of common values for this structural parameter could suggest that (i) this parameter is not fundamental for the activity; (ii) the two negatively charged moieties could move to adopt the same conformation near the receptor; (iii)

each antagonist could be active with two negatively charged groups, separated by a distance ranging from 3 to 7.5 Å.

In agreement with the last assumptions, and given that the distance separating two carboxylate moieties complexing a divalent calcium cation ranges from 3.02 to 11.61 Å in all protein structures containing a calcium ion found in the Protein Data Bank of the Brookhaven National Laboratory, we suggest that the two negatively charged groups present in all studied antagonists might bind the $\alpha_{IIb}\beta_3$ integrin by chelating one of the four calcium cations present on the α_{IIb} glycoprotein. This assumption is consistent with the Ca^{2+} dependence of the ligand binding activity of the $\alpha_{IIb}\beta_3$ integrin [37].

In addition, among the four known divalent cation binding sites on the α_{IIb} subunit [38], one of them, called B12 [32], is cross-linked by the fibrinogen γ chain [12]. The binding between the dodecapeptide C-terminus of the fibrinogen γ chain and the B12 site in α_{IIb} could be one of the binding mechanism involved in the fibrinogen/platelet adhesion, and in the vWF/platelet adhesion, because their recognition mechanisms with regard to the C-terminus of the human fibrinogen γ chain are the same [10].

Hypothetical part

The presence of hydrophobic groups in the core of the four non-peptide antagonists (**1**–**4**), which are the most potent of the six studied compounds, might enhance the binding to $\alpha_{IIb}\beta_3$ by shielding the charged groups from the solvent interactions. This assumption was already made with RGD-containing peptides and disintegrins [39]. The conformational studies of RGD-based $\alpha_{IIb}\beta_3$ antagonists, however, could not give accurate values of the distance separating the charged groups. This is due to the flexibility of the side chains of the aspartic acid and the arginine amino acids [40, 41]. Nevertheless, the 'cup-shaped' structure between the ionic functional groups seems to be a requirement in RGD-based antagonists to reach a high potency [42]. Our theoretical approach leads to the same conclusion for not only two charged groups, but for three. It was established that RGD interacts with the β_3 chain [43], and the dodecapeptide C-terminus of the fibrinogen γ chain, with the α_{IIb} chain [12]. This study may suggest that compounds (**1**) to (**5**) interact with the same binding site(s) as the dodecapeptide, and this assumption could explain the selectivity of these

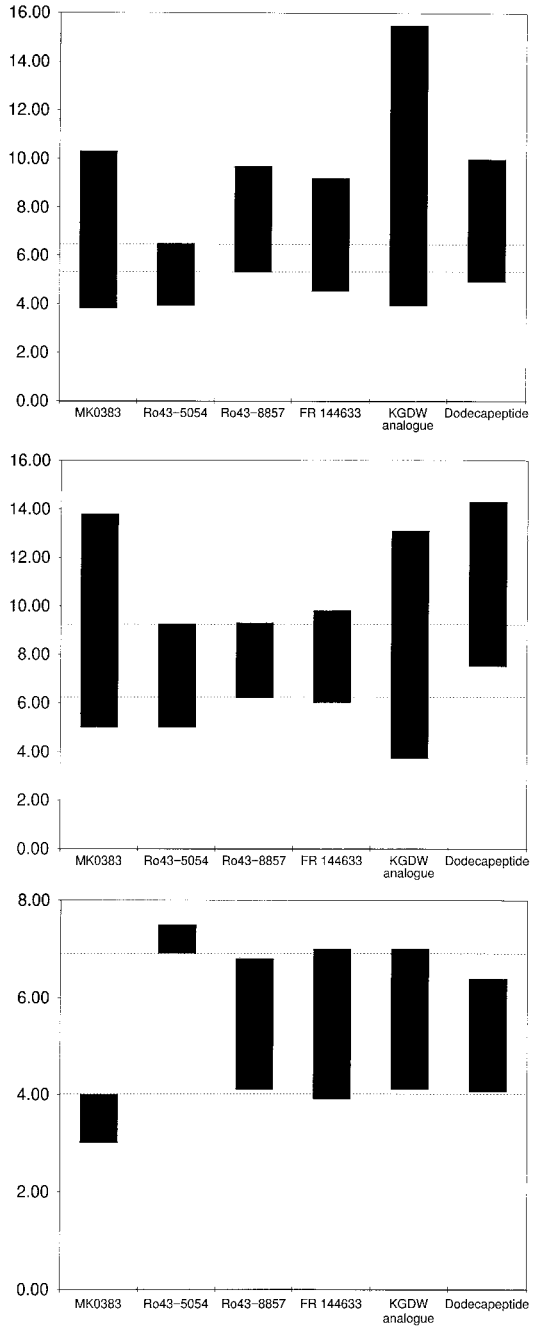

Figure 3. Top. Comparisons between the distances (in Å) separating the positively charged moiety and one carboxylate or sulfone moiety (numbered (**1**) in Figure 1, or Cγ of Asp^{410} for the dodecapeptide) during the dynamics trajectories. Middle. Comparisons between the distances (in Å) separating the positively charged moiety and the other carboxylate moiety (numbered (**2**) in Figure 1, or C-terminus of Val^{411} for the dodecapeptide) during the dynamics trajectories. Bottom. Comparisons between the distances (in Å) separating the two negatively charged moieties (numbered (**1**) and (**2**) in Figure 1, or Cγ of Asp^{410} and C-terminus of Val^{411} for the dodecapeptide) during the dynamics trajectories.

compounds. In addition, other non-peptide selective antagonists of $\alpha_{IIb}\beta_3$ possessing only one negatively charged moiety, such as BIBU 52 from Karl Thomae [44] or GR 144043 from Glaxo [45], and having all IC_{50} values in the nanomolar range, may interact in a selective manner with the β_3 chain, and not with α_{IIb}, i.e. with the binding site of the RGD sequence. Thus, the existence of two possible binding sites in the integrin $\alpha_{IIb}\beta_3$ may allow to block it by selectively inhibiting at least one of the two sites. It was recently suggested that the dodecapeptide C-terminus of the fibrinogen γ chain interacts at two different binding sites, and competes with RGD for one of them [46]. The fact that our theoretical approach leads to a 'cup shaped' structure between charged moieties in the conformations of the antagonists, just like the one found for RGD-based antagonists, suggests that molecules (**1**)–(**5**) can bind both to the RGD binding site and to the binding site of the dodecapeptide C-terminus of the fibrinogen γ-chain. One negatively charged and one positively charged group of each studied antagonist (**1**)–(**5**) could mimic the aspartic acid and arginine side chains binding the β_3 chain, whereas the second negatively charged group could interact selectively with the α_{IIb} chain in the other binding site.

An additional parameter reinforced this hypothesis: when the amino acid following the RGD sequence possesses a hydrophobic side chain, the anti-aggregatory activity is further enhanced [47, 48]. This is in agreement with our theoretical pattern, where a hydrophobic group is placed near the negatively charged moieties. The remaining question is then: which negatively charged moiety, N_1 or N_2, could mimic the Asp side chain? To try to address this issue, we analysed the distances separating the C_ζ carbon of the arginine and the C_γ atom of the aspartic acid in all the crystal structures found in a representative list of Protein Data Bank chain identifiers (March 1997) [49] presenting the RGD fragment. Only 48 structures were found, and among them, one possessed a distance falling in the P_1–N_1 space and six possessed a distance falling in the P_1–N_2 space, according to the notation of Figure 4 (data not shown). We therefore, could not attribute the Asp mime to N_1 or N_2. In addition, structures of the antagonists (**1**)–(**6**) may be different in the two binding sites.

The fact that the $\alpha_v\beta_3$ binding site is less flexible and wide than the $\alpha_{IIb}\beta_3$ binding site [40] could exclude the insertion of the specific $\alpha_{IIb}\beta_3$ antagonist binding sequence, composed of three charged moieties or too rigid and too wide, in the $\alpha_v\beta_3$ binding pocket, and allows it in the $\alpha_{IIb}\beta_3$ binding site, with a high affinity, with regard to the previous considerations about the possible interactions between $\alpha_{IIb}\beta_3$ and their ligands.

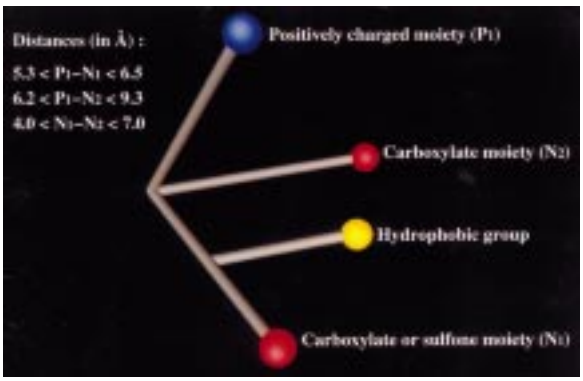

Figure 4. Theoretical pattern of the five studied non-peptide $\alpha_{IIb}\beta_3$ selective antagonists.

Conclusions

The results shown here may suggest that, whereas the strategies used to develop some selective $\alpha_{IIb}\beta_3$ antagonists are different, these compounds all present a similar structure in solution, presumed to be closely related to their bound conformation. RGD and the dodecapeptide sequences binding $\alpha_{IIb}\beta_3$ in a mutually competitive manner [50], it can be hypothesised that they have, at least one common binding site. The lower flexibility and width of other integrin RGD dependent binding pocket (including $\alpha_v\beta_3$), however, could not allow the penetration of the dodecapeptide C-terminus part, but only of the smaller RGD sequence. This could, thus, be an explanation of the specificity of the antagonists studied here, that seem to mimic the C-terminus part of the fibrinogen γ chain. Using the common structure found for all these molecules, new oral potentially active $\alpha_{IIb}\beta_3$ carbohydrate-based inhibitors are currently designed and will be described in a forthcoming paper [51].

Another important challenge will be to elucidate the three dimensional structure of the $\alpha_{IIb}\beta_3$ integrin and of its binding pocket(s), to provide novel insights into the mechanism of integrin ligand interactions.

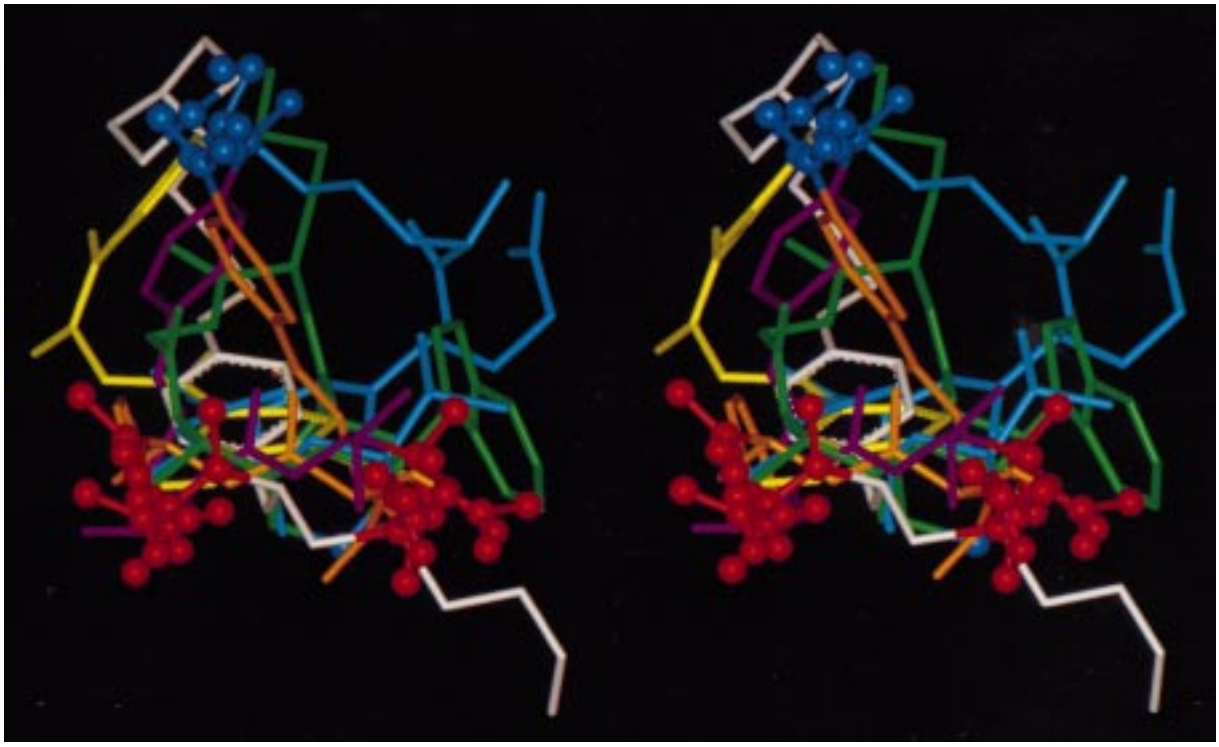

Figure 5. (**1**), (**2**), (**3**), (**4**), (**5**) and (**6**) superimposed; molecules are coloured according to the following scheme: (**1**) white, (**2**) orange, (**3**) yellow, (**4**) purple, (**5**) green, and (**6**) blue. The positive moieties are coloured blue, carboxylate and sulfone moieties are coloured red. For clarity, only the six last amino acid residues (KQAGDV) of **(6)** are drawn.

Acknowledgements

Computer resources were provided in part by the Centre Charles Hermite, in Nancy. HM is indebted to the Laboratoire de Chimie Théorique de Nancy for his doctoral fellowship. Christophe Chipot is thanked for a critical reading of the original manuscript.

References

1. Phillips, D.R., Charo, I.F., Parsie, L.V. and Fitzgerald, L.A., Blood, 71 (1988) 831.
2. Marguerie, G.A., Plow, E.F. and Edington, T.S., J. Biol. Chem., 254 (1979) 5357.
3. Coller, B.S., N. Engl. J. Med., 322 (1990) 33.
4. Jakubowski, J.A., Smith, G.F. and Sall, D.J., Annu. Rep. Med. Chem., 27 (1992) 99.
5. Plow, E.F., Piersbacher, M.D., Ruoslahti, E., Marguerie, G.A. and Ginsberg, M.H., Proc. Natl. Acad. Sci. USA, 82 (1985) 8057.
6. Gartner, T.K. and Bennet, J.S., J. Biol. Chem., 260 (1985) 11891.
7. Hawiger, J., Kloczewiak, M., Bedmarek, M.A. and Timmons, S., Biochemistry, 28 (1989) 2909.
8. Plow, E.F., D'Souza, S.E. and Ginsberg, M.H., Sem. Thromb. Haemostas., 18 (1992) 324.
9. Kloczewiak, M., Timmons, S., Lukas, T.J. and Hawiger, J., Biochemistry, 23 (1984) 1767.
10. Timmons, S., Kloczewiak, M. and Hawiger, J., Proc. Natl. Acad. Sci. USA, 81 (1984) 4935.
11. Plow, E.F., Srouji, A.H., Meyer, D., Marguerie, G. and Ginsberg, M.H., J. Biol. Chem., 259 (1984) 5388.
12. D'Souza, S.E., Ginsberg, M.H., Burke, T.A. and Plow, E.F., J. Biol. Chem., 265 (1990) 3440.
13. Weller, T., Alig, L., Müller, M.H., Kouns, W.C. and Steiner, B., Drugs Future, 19 (1994) 461.
14. Gehlsen, K.R., Davis, G.E. and Sriramarao, P., Clin. Exp. Metastasis, 10 (1992) 111.
15. Hart, I.R., Birch, M. and Marshall, J.F., Cancer Metastasis Rev., 10 (1991) 115.
16. Davies, J., Warwick, J., Totty, N., Philp, R., Helfrich, M. and Horton, M., J. Cell. Biol., 109 (1989) 1817.
17. Lakkakorpi, P.T., Horton, M.A., Helfrich, M., Karhukorpi, E.K. and Vaanonen, H.K., J. Cell. Biol., 115 (1991) 1179.
18. Nikiforovich, G.V., Int. J. Pept. Protein Res., 44 (1994) 513.
19. Computational results obtained using software from Biosym/MSI (San Diego, CA) – dynamics calculations and minimizations were done with the *Discover*® program, using CVFF forcefield, ab initio calculations were done with the *AMPAC*® / *MOPAC*® program and graphical displays were printed out from the *Insight*® *II* molecular modelling system.
20. Kirkpatrick, S., Gelatt, C.D. and Vechi, M.P., Science, 220 (1983) 671.
21. Verlet, L., Phys. Rev., 159 (1967) 98.

22. Berendsen, H.J.C., Postma, J.P.M., van Gunsteren, W.F., DiNola, A. and Haak, J.R., J. Chem. Phys., 81 (1984) 3684.
23. Cotrait, M., Kreissler, M., Hoflack, J., Lehn, J.-M. and Maigret, B., J. Comput.-Aided. Mol. Design, 6 (1992) 113.
24. Greenspoon, N., Hershkoviz, R., Alon, R., Varon, D., Shenkman, B., Marx, G., Federman, S., Kapustina, G. and Lider, O., Biochemistry, 32 (1993) 10001.
25. Gould, R.J., Chang, C., Lynch, R.J., Manno, P.D., Zhang, G., Bednar, B., Friedman, P.A., Egbertson, M., Turchi, L.M., Anderson, P.S. and Hartman, G., Thrombos. Haemostas., 69 (1993) 976.
26. Hartman, G.D., Egbertson, M.S., Halczenko, W., Laswell, W.L., Duggan, M.E., Smith, R.L., Naylor, A.M., Manno, P.D., Lynch, R.J., Zhang, G., Chang, C.T.-C. and Gould, R.J., J. Med. Chem., 35 (1992) 4640.
27. Alig, L., Edenforder, A., Hadváry, P., Hürzeler, M., Knopp, D., Müller, M., Steiner, B., Trzeciak, A. and Weller, T.J., J. Med. Chem., 35 (1992) 4393.
28. Cox, D., Aoki, T., Seki, J. and Motoyama, Y., Thrombos. Haemostas., 69 (1993) 706.
29. Fauchère, J.-L., Morris, A.D., Thurieau, C., Simonet, S., Verbeuren, T. and Kieffer, N., Int. J. Pept. Protein Res., 42 (1993) 440.
30. Scarborough, R.M., Rose, J.W., Naughton, M.A., Phillips, D.R., Nannizzi, L., Arfsten, A., Campbell, A.M. and Charo, I.F., J. Biol. Chem., 268 (1993) 1058.
31. Scarborough, R.M., Naughton, M.A., Teng, W., Rose, J.W., Phillips, D.R., Nannizzi, L., Arfsten, A., Campbell, A.M. and Charo, I.F., J. Biol. Chem., 268 (1993) 1066.
32. D'Souza, S.E., Ginsberg, M.H., Matsueda, G.R. and Plow, E.F., Nature, 350 (1991) 66.
33. Mulliken, R.S., J. Chem. Phys., 23 (1955) 1833, 1848, 2338, 2343.
34. Donahue, J.P., Patel, H., Anderson, W.F. and Hawiger, J., Proc. Natl. Acad. Sci. USA, 91 (1994) 12178.
35. Mayo, K.H., Burke, C., Lindon, J.N. and Kloczewiak, M., Biochemistry, 29 (1990) 3277.
36. Scarborough, R.M., Rose, J.W., Hsu, M.A., Phillips, D.A., Fried, V.A., Campbell, A.M., Nannizzi, L. and Charo, I.F., J. Biol. Chem., 226 (1991) 9359.
37. Gulino, D., Boudignon, C., Zhang, L., Concord, E., Rabiet, M.-J. and Marguerie, G., J. Biol. Chem., 267 (1992) 1001.
38. Phillips, D.R., Charo, I.F. and Scarborough, R.M., Cell, 65 (1991) 359.
39. McDowell, R.S. and Gadek, T.R., J. Am. Chem. Soc., 114 (1992) 9245.
40. Pfaff, M., Tangemann, K., Müller, B., Gurrath, M., Müller, G., Kessler, H., Timpl, R. and Engel, J., J. Biol. Chem., 269 (1994) 20233.
41. McDowell, R.S., Blackburn, B.K., Gadek, T.R., McGee, L.R., Rawson, T., Reynolds, M.E., Robarge, K.D., Somers, T.C., Thorsett, E.D., Tischler, M., Webb II, R.R. and Michael, C.V., J. Am. Chem. Soc., 116 (1994) 5077.
42. McDowell, R.S., Gadek, T.R., Barker, P.L., Burdick, D.J., Chan, K.S., Quan, C.L., Skelton, N., Struble, M., Thorsett, E.D., Tischler, M., Tom, J.Y.K., Webb, T.R. and Burnier, J.P., J. Am. Chem. Soc., 116 (1994) 5069.
43. D'Souza, S.E., Ginsberg, M.H., Burke, T.A., Lam, S.C.-T. and Plow, E.F., Science, 242 (1988) 91.
44. Muller, T.H., Weisenberger, H., Brickl, R., Narjes, H., Himmelsbach, F. and Krause, J., Circulation, 96 (1997) 1130.
45. Eldred, C.D., Evans, B., Hindley, S., Judkins, B.D., Kelly, H.A., Kitchin, J., Lumley, P., Porter, B., Ross, B.C. and Smith, K.J., J. Med. Chem., 37 (1994) 3882.
46. Mayo, K.H., Fan, F., Beavers, M.P., Eckardt, A., Keane, P., Hoekstra, W.J. and Andrade-Gordon, P., Biochemistry, 35 (1996) 4434.
47. Gurrath, M., Müller, B., Kessler, H., Aumailley, M. and Timpl, R., Eur. J. Biochem., 210 (1992) 911.
48. Seetharam, D.S.J., Usman, S.F.T., Soma, C. and Teruna, J.S., J. Biomol. Struct. Dyn., 14 (1996) 1.
49. Hobohm, U. and Sander, C., Protein Sci., 3 (1994) 522.
50. Lam, S.C.-T., Plow, E.F., Smith, M.A., Andrieux, A., Ryckwaert, J.J., Marguerie, G. and Ginsberg, M.H., J. Biol. Chem., 262 (1987) 947.
51. Moitessier, N., Minoux, H., Maigret, B., Chrétien, F. and Chapleur, Y., Lett. Pept. Sci., 5 (1998) 75.